

Superposition Enhanced Nested Sampling

Stefano Martiniani^{†,*}, Jacob D. Stevenson,[†] David J. Wales, and Daan Frenkel

University Chemical Laboratories, University of Cambridge, Lensfield Road, Cambridge CB2 1EW, UK

(Dated: June 3, 2014)

The theoretical analysis of many problems in physics, astronomy and applied mathematics requires an efficient numerical exploration of multimodal parameter spaces that exhibit broken ergodicity. Monte Carlo methods are widely used to deal with these classes of problems, but such simulations suffer from a ubiquitous sampling problem: the probability of sampling a particular state is proportional to its entropic weight. Devising an algorithm capable of sampling efficiently the full phase space is a long-standing problem. Here we report a new hybrid method for the exploration of multimodal parameter spaces exhibiting broken ergodicity. Superposition enhanced nested sampling (SENS) combines the strengths of global optimization with the unbiased/athermal sampling of nested sampling, greatly enhancing its efficiency with no additional parameters. We report extensive tests of this new approach for atomic clusters that are known to have energy landscapes for which conventional sampling schemes suffer from broken ergodicity. We also introduce a novel parallelization algorithm for nested sampling.

I. INTRODUCTION

Computer simulations play an important role in the study of phase transitions and critical phenomena. In particular, stochastic techniques such as Monte Carlo (MC) methods have proved to be powerful tools [1]. These methods rely on the ability of the Monte Carlo algorithm to sample the accessible volume in phase space. There are, however, many situations where standard Monte Carlo simulations suffer from a lack of ergodicity. In that case, more sophisticated algorithms are needed to explore the volume in phase space that is, in principle, accessible. Some such techniques are based on the efficient exploration of the underlying, multi-dimensional potential energy surface (PES) [2]. The PES, or energy landscape, can be viewed as a collection of basins separated by barriers, where each basin corresponds to a particular local minimum-energy configuration. The basin volumes define the entropic weight of the corresponding local minima. The transition rate from one basin to another depends on the barrier height as well as the relative entropic weights (configurational space volumes) [2]. Many PES of interest exhibit frustration in the form of low-lying minima with different morphologies separated by high barriers. These structures may act as kinetic traps, when fixed-temperature sampling methods such as molecular dynamics or Metropolis Monte Carlo sampling are used. There exist a wide range of extended or biased sampling techniques, both in Monte Carlo and in Molecular Dynamics, that make it possible to speed up the sampling of landscapes with kinetic traps. These techniques include Monte Carlo methods, such as umbrella sampling [3, 4], density of states based methods, such as the Wang-Landau method [5] and replica exchange methods [6, 7], along with their Molecular Dynamics counterparts. Examples are the replica-exchange

MD method [8], and the Meta-Dynamics method [9]. In cases where a biased distribution is generated, the original distribution can be reconstructed using reweighting techniques [10, 11]. However, these approaches may perform poorly when dealing with high-dimensional spaces exhibiting broken ergodicity or, in other words, with highly multimodal (or multifunnel [2, 12–14]) parameter spaces [15–18].

In recent years a Bayesian method known as nested sampling [19] has emerged as a possible alternative to extended or biased sampling methods. The nested-sampling approach has found widespread application in astrophysics [20, 21] and cosmology [22, 23], and has drawn the attention of computational and statistical physicists [24–29]. Furthermore, the method has been recently adopted for Bayesian model comparison in systems biology [30–32]. Nested sampling explores phase space in an unbiased way, and allows one to determine statistically the density of states associated with shrinking fractions of phase space. This objective is achieved by placing a constraint on the potential energy (for instance), which decreases at each nested sampling iteration. Like Wang-Landau sampling, the method is athermal and produces the density of states and the partition function (Bayesian evidence) as its primary product. However, nested sampling does not require binning of the energy for systems with continuous potentials. The self-adapting steps in energy (but constant in log phase space volume) is attractive because the approach does not require prior knowledge of possible phase transitions. For example, the step size adjusts automatically as the phase space volume shrinks near a first order phase transition [19, 25].

An important drawback of nested sampling is that when the decreasing energy constraint forbids a transition to an unexplored basin, that basin cannot be visited and ergodicity is broken. Hence, while nested sampling certainly is conceptually interesting, its performance is often no better than that of conventional extended sampling methods in dealing with systems exhibiting broken

* sm958@cam.ac.uk; Corresponding author

[†] These authors have contributed equally to this work

ergodicity [25]. In the present work we introduce a novel hybrid methodology for the exploration and thermodynamic analysis of such systems.

Superposition enhanced nested sampling (SENS) combines the strengths of unbiased global optimization techniques [2] with those of nested sampling. Global optimization techniques such as basin-hopping [33–35] are designed to find the lowest energy configuration of a PES. They are not constrained to sample according to any distribution, so they are free to use ‘quick and dirty’ techniques while searching for the global minimum. For example, they can take Monte Carlo steps that do not satisfy detailed balance, and make use of minimisation algorithms such as L-BFGS and conjugate gradient. Such operational freedom makes global optimization algorithms much more efficient than generalised ensemble methods at locating the lowest energy minima [36–40]. Collections of the lowest energy minima configurations thus obtained can then be used in the context of the superposition approach (SA) [2, 39–45] to compute the thermodynamic properties of the system. However, doing so accurately at high temperatures using the SA alone often requires a prohibitively large number of minima.

In the present contribution we show how knowledge of the lowest energy minima and their statistical weights, calculated using the harmonic superposition approximation (HSA), can be exploited to enhance the problematic low energy behaviour of nested sampling, thus making it likely that none of the important minima and associated regions are missed. Although we discuss SENS in the context of energy landscapes, the method is completely general and can be applied to any multi-modal parameter space whose minima (maxima in likelihood) can be identified by global optimization algorithms.

NESTED SAMPLING

Nested sampling [19] provides an elegant solution to the problem of evaluating the density of states, and hence the partition function, for arbitrary systems. A likelihood value is assigned to each possible configuration. For our purposes the likelihood is the Boltzmann factor $\exp(-E/k_B T)$, but it could be some other measure. Typically, there are large numbers of configurations with a low likelihood. In addition, there may be a small number of configurations with high likelihood.

The aim of nested sampling is to sample configuration space uniformly, but with the energy constrained to lie below a maximum value, E^{max} , that decreases iteratively throughout the calculation. The rate of decrease is maintained self-consistently, such that the phase space volume with energy less than E^{max} decreases by a constant factor in each iteration.

The nested sampling algorithm starts by generating K configurations of the system completely at random, distributed uniformly, in configuration space. The energy, $E_{\mathcal{R}}$, of each of these configurations is computed

and added to a sorted list, where \mathcal{R} is the associated index in the sorted list. For each of these replicas we define the configurational phase space volume, $\Omega_{E \leq E_{\mathcal{R}}}$, containing all configurations with $E \leq E_{\mathcal{R}}$. The key insight of nested sampling is that the volumes, $\Omega_{E \leq E_{\mathcal{R}}}$, normalised by the total phase space volume, are distributed according to the Beta distribution, $\text{Beta}(K - \mathcal{R} + 1, \mathcal{R})$ [46]. This distribution has expectation value and variance

$$\mu_{\mathcal{R}} = 1 - \frac{\mathcal{R}}{K + 1} \quad \text{and} \quad \sigma_{\mathcal{R}}^2 = \frac{\mathcal{R}(K - \mathcal{R} + 1)}{(K + 2)(K + 1)^2}. \quad (1)$$

The above formalism assumes that the total phase space volume Ω_{tot} is finite, but this condition can generally be satisfied with negligible error, for example by placing the system in a large box.

At the i -th nested sampling iteration the replica (out of K replicas) with highest energy E_i^{max} is discarded and replaced by a new configuration sampled uniformly under the constraint $E \leq E_i^{max}$. The maximum energy E_i^{max} is stored for later analysis. Again, the volume of configuration space with energy less than the \mathcal{R} -th largest energy, $\Omega_{E \leq E_{\mathcal{R}}}$, this time normalized by $\Omega_{E \leq E_i^{max}}$, is distributed according to the Beta distribution with mean and variance given by Eq. (1). During the nested sampling iteration the volume of phase space with energy below E^{max} contracts, on average, by $\mu_1 = K/(K + 1)$. After N nested sampling iterations, the algorithm produces a list of the form $\{E_1^{max}, E_2^{max}, \dots, E_N^{max}\}$. We can associate a fraction of configuration space $X_i = \Omega_{E \leq E_i^{max}}/\Omega_{tot} = \mu_1^i$, with each E_i^{max} . The density of states, or the (normalized) volume of phase space with energy between E_{i+1}^{max} and E_i^{max} is simply

$$g_i(E) = X_i - X_{i+1} = \mu_1^i - \mu_1^{i+1} = \frac{1}{K + 1} \left(\frac{K}{K + 1} \right)^i. \quad (2)$$

Thermodynamic quantities of interest, such as the mean energy, entropy, free energy, and heat capacity, can easily be computed from the density of states at arbitrary temperature.

To generate configurations uniformly in space we use the strategy suggested by Skilling [19]: after removing the configuration with highest energy one of the remaining $K - 1$ replicas (chosen randomly) is duplicated. The new configuration is then evolved through a Markov chain Monte Carlo (MCMC) walk sufficiently long to decorrelate the system from its initial state. This Monte Carlo walk is equivalent to a normal Monte Carlo simulation at infinite temperature. The coordinates are randomly perturbed, and the new configuration is accepted subject only to the condition that the energy remains below E^{max} . For most systems of interest the vast majority of the computational effort will be spent generating new configurations.

Parallelization

Nested sampling can be formulated to run in parallel on an arbitrary number of processors. We present a pseudocode description of our parallel implementation in Algorithm 2. Since this scheme also constitutes the basic framework for SENS we define the MCMC loop in the most general way at line 9 of Algorithm 2. For the purpose of discussing the algorithm in its simplest form here we will consider Algorithm 1.

```

for  $l = 0$  to  $N$ -steps do
  generate trial configuration (e.g. by random
  perturbation);
  if  $E_{trial} \leq E_{max}$ : accept trial configuration;
end for

```

ALGORITHM 1. Nested sampling MCLoop

At each nested sampling iteration, instead of removing only the replica with the highest energy, we remove the \mathcal{P} replicas with highest energy, where \mathcal{P} is the number of processors available. The rate of phase space contraction now is given by $\mu_{\mathcal{P}}$, leading to much faster phase space contraction and shorter calculations in terms of wall-clock time. This parallelization procedure was first described in reference [27]. Our improvement is that we do not discard the $\mathcal{P} - 1$ replicas with highest energy but we store them for later analysis. Phase space contraction between iterations is still constant, but now the post-analysis is slightly more complicated. The fraction of configuration space associated with the n -th recorded energy is

$$X_n = \prod_{i=0}^n \frac{K - i\% \mathcal{P}}{K + 1 - i\% \mathcal{P}}, \quad (3)$$

where “%” is the mod operator. This method follows the same stepping routine as the existing parallelization algorithm. However it produces \mathcal{P} times as many points, hence providing a more detailed picture of the potential energy surface and a much more fine-grained binning of the density of states.

SENS - THE CONCEPT

Global optimization is a common numerical problem and global optimization algorithms have been developed in many areas of science [2, 47, 48]. Knowledge of the local minima alone, however, is not sufficient to infer all the observable properties of interest from the energy landscape (or in general any parameter space). The harmonic superposition approximation (HSA) [49] (for more details, see e.g. [2]) allows one to compute the density of states and the partition function, solely based on the knowledge of the individual local minima and the local curvatures (normal mode frequencies) of the potential energy landscape, via the Hessian matrix. In the HSA each

```

   $\triangleright$  initialisation
1: generate  $K$  random configurations;
2: store their coordinates and energy in LiveList ;
   $\triangleright$  main loop
3: while termination condition is False do
4:   remove the  $\mathcal{P}$  replicas  $\{\mathbf{R}_m^{(1)}, \dots, \mathbf{R}_m^{(\mathcal{P})}\} \equiv \{\mathbf{R}_m\}$ 
   with highest energy  $\{E_m^{(1)} > \dots > E_m^{(\mathcal{P})}\} \equiv \{E_m\}$ 
   from LiveList ;
5:   append  $\{E_m\}$  to OutputList ;
6:   set  $E_{max} = E_m^{(\mathcal{P})}$ ;
7:   select  $\mathcal{P}$  replicas  $\{\mathbf{R}_s^{(1)}, \dots, \mathbf{R}_s^{(\mathcal{P})}\} \equiv \{\mathbf{R}_s\}$  from
   LiveList at random;
8:   add a copy of  $\{\mathbf{R}_s\}$  to LiveList ;
9:   MCLoop $\{\{\mathbf{R}_s\}, E_{max}, \text{minima.db}\}$ 
10: end while

```

ALGORITHM 2. Parallel nested sampling

local minimum corresponds to a harmonic basin and observable properties are expressed as a sum over individual contributions of the minima.

The HSA has been shown to be very effective for several systems [18, 40, 50] but the accuracy depends on how well the potential energy of the basins can be approximated as harmonic, and how many minima are thermodynamically important. While the HSA captures landscape anharmonicity, arising from the distribution of local minima, it does not include well anharmonicity, arising from the shape of the well. Therefore, the HSA becomes an increasingly good approximation at lower energies where well anharmonicity is less important. The total number of minima increases exponentially with system size [49, 51], but it is impossible to tell a-priori how many of those are important. For example, LJ₃₁, a cluster of 31 isotropic particles interacting through a Lennard-Jones potential [52], has about 3×10^{15} distinct minima [12], but only a few dozen are required to reproduce the low temperature thermodynamic behaviour.

The global resolution of nested sampling depends on the number of replicas, K , used in the simulation, which is generally limited by the available computation time (the larger K , the slower the descent in energy). A more serious problem for nested sampling is that if the barrier to enter an unexplored funnel or superbasis is higher than the energy constraint E_{max} , that region of the PES will never be explored if it is not already populated. For example, in a crystallisation transition, at high energy the statistical weight of the liquid phase will be overwhelming and there will be no replicas in the region corresponding to the solid phase. However, as the energy constraint decreases (hence the temperature) the relative statistical weight associated with the solid phase increases. If we could sample phase space uniformly then at low energy we would observe a phase transition corresponding to crystallisation, but we must resort to a MCMC walk to explore phase space. If the entrance to the superbasis corresponding to the crystal has been locked out by E_{max} a Markov chain will not be able to find it, thus missing

the transition.

Here we propose a new method that combines complementary techniques: nested sampling can sample efficiently the high energy regions of phase space, while at low energy a database of minima obtained by global optimization is used to augment the survey. While nested sampling assigns the correct statistical weight to each basin, global optimization makes it likely that no important minima are missed. This philosophy is also used in other methods combining replica exchange Monte Carlo with global optimization algorithms to treat broken ergodicity [12, 16, 53, 54].

SENS - THE ALGORITHM

Employing knowledge of low-lying minima fits naturally within the framework of nested sampling. We present here both an exact and an approximate implementation of the SENS algorithm. Exact SENS is fully unbiased and requires no additional parameters than those needed in nested sampling. Approximate SENS, on the other hand, is formally biased and requires additional parameters. The reason for presenting both methods is that, in some cases, the latter approach can be considerably simpler to implement than the former, while generally producing equally good, or better, results. SENS is based on the original nested sampling algorithm presented in Algorithm 2. The novelty of our method resides in the augmented sampling of the parameter space obtained by coupling the MCMC to the HSA. SENS can therefore be implemented by changing the function `MCLoop` ($\{\mathbf{R}_s\}$, E_{max} , `minima.db`) of Algorithm 2. A full outline of the SENS algorithm can be found in Algorithm 3 of the Supplementary Information. To run SENS, a database of the lowest energy minima must be pre-computed.

In this work we adopt basin-hopping [33–35] as the global optimization algorithm of choice. Basin-hopping associates any given point of the PES to a minimum obtained by energy minimisation, thus transforming the PES into a set of catchment basins. This basin transformation is combined with a sampling scheme to search for the global minimum. At each step the coordinates of the current minimum configuration are perturbed to hop out the basin and minimised again to find a new minimum. Each step between two minima configurations is accepted with probability

$$P(\mathbf{x}_{old} \rightarrow \mathbf{x}_{new}) = \min[1, \exp(-\beta(E_{new} - E_{old}))].$$

If the move is rejected, the coordinates are reset to those of the current local minimum. Since perturbations should be large enough to step out of the catchment basin, the step-size is typically much larger than for thermodynamic sampling. Furthermore, since detailed balance need not hold, the step-size can be dynamically adjusted to improve sampling. Basin-hopping has been successfully ap-

plied to a wide range of atomic, molecular, soft and condensed matter systems [50, 55–57].

Exact SENS

An unbiased version of SENS can be implemented by means of Hamiltonian replica exchange Monte Carlo moves [58, 59]: in addition to normal MC steps, we introduce a new Monte Carlo step in which a minimum is sampled from the database according to its HSA configurational entropic weight:

$$w_c^{(b)}(E) = \frac{\Omega_c^{(b)}(E)}{\Omega_c(E)}. \quad (4)$$

We define the configurational volume of basin b

$$\Omega_c^{(b)}(E) \propto \frac{n_b(E - V^{(b)})^{\frac{\kappa}{2}}}{\prod_{\alpha=1}^{\kappa} \nu_{\alpha}^{(b)}}, \quad (5)$$

and the total configurational volume

$$\Omega_c(E) \propto \sum_b \frac{n_b(E - V^{(b)})^{\frac{\kappa}{2}}}{\prod_{\alpha=1}^{\kappa} \nu_{\alpha}^{(b)}}, \quad (6)$$

where $V^{(b)}$ is the potential energy of the minimum corresponding to basin b , $\nu_{\alpha}^{(b)}$ are the normal mode vibrational frequencies defined by the Hessian matrix, κ is the number of vibrational degrees of freedom, and n_b is the degeneracy of the basin (for Lennard-Jones clusters this is the number of distinct non-superimposable permutation-inversion isomers for minimum b) [2]. Here we have left out all the constant factors that cancel out as well as overall rotations. Once a minimum is selected, a configuration with $E \leq E_{max}$ is then chosen uniformly from within its basin of attraction. This approach corresponds to selecting a point uniformly from a multidimensional harmonic well. Such a configuration can be generated analytically, see the Supplementary Information for details. Unlike Ref. [16], in our approach we sample from the uniform distribution of configurations below energy E_{max} , rather than from the corresponding canonical distribution.

Thus, we obtain a configuration \mathbf{R}_{sys} sampled according to the true Hamiltonian, \mathbb{H}_{sys} , and a trial configuration, \mathbf{R}_{har} , sampled according to the HSA-Hamiltonian, \mathbb{H}_{har} . The energies of the two configurations are then computed with the other Hamiltonian. If

$$\mathbb{H}_{har}(\mathbf{R}_{sys}) \leq E_{max} \text{ and } \mathbb{H}_{sys}(\mathbf{R}_{har}) \leq E_{max}, \quad (7)$$

then the true distribution and the HSA distributions overlap, the swap is accepted, and \mathbf{R}_{sys} becomes \mathbf{R}_{har} , otherwise it is rejected. This procedure guarantees that detailed balance is satisfied, for further discussion refer to the Supplementary Information. In practice only the lowest energy minima will successfully swap, since the HSA

can only be reasonably accurate around these basins. It is, however, at low energy that such swaps are needed the most due to the hard energy constraint used by nested sampling. Note that swaps are complemented by regular MCMC walks to allow for the exploration of the full configuration space. In SENS the replicas are allowed to “tunnel” between basins, thus improving the sampling. A more detailed description, along with a pseudo-code implementation of MCLoop specific to Lennard-Jones clusters is provided in the Supplementary Information.

Approximate SENS

The implementation of approximate SENS is somewhat simpler, but comes at the cost of at least one extra parameter. The basic idea of approximate SENS is that the sampling of configuration space can be augmented by starting a MCMC walk from a local minimum configuration, sampled from the database according to its entropic weight Eq. (4), with some user defined frequency. This frequency is intrinsically defined in exact SENS by the relative overlap of the HSA and the true density of states. To implement approximate SENS we only need a database of minima and their relative weights computed according to Eq. (4). Before each MCMC step a random number is drawn. If this number is less than some user defined probability, P_{DS} , then a minimum is selected from the database according to the HSA weights and the MCMC walk starts from this minimum configuration. A pseudo-code implementation of MCLoop for approximate SENS is provided in the Supplementary Information.

There are two main sources of bias in the approximate SENS. The first one is due to the limited number of minima from which we sample, since we cannot include the large number of high energy minima. The second source of error is due to the poor quality of the HSA approximation far from the minimum, hence the entropic weights for the minima are not accurate at high energy. The most obvious way of reducing these biases is to use long MCMC walks. In fact, if we sample from the wrong basin a long MCMC walk will allow the system to escape and explore regions of phase space with greater entropic weight. However, very long MCMC walks are computationally expensive, and if short runs are required we need to sample from the database of minima carefully. If we start sampling from the database of minima at high energy we will possibly introduce a bias due to over-weighting of the low energy regions of configuration space. To avoid this problem we suppress sampling from the database until we are sure the HSA is likely to describe the potential energy landscape accurately. We use a simple function (of the Fermi type) that delays the onset of sampling from the database of minima and limits its maximum frequency

$$f_{onset} = \frac{f_{max}}{1 + e^{(E_{min}^{(\mathcal{R})} - E_{on})/\Delta E}}, \quad (8)$$

where E_{on} is some onset energy and $E_{min}^{(\mathcal{R})}$ is the en-

ergy of the replica with lowest energy. E_{on} could be chosen as $E_{max}^{(\text{minima.db})}$, the energy of the highest known minimum (stored in the database), or as the largest energy at which the HSA describes the system accurately. f_{max} and ΔE are user-defined parameters that determine the total probability of sampling after the onset and the width of the onset region, respectively. For small sampling probabilities, $P_{DS} \ll 1$, the optimal frequency of sampling from the database, should scale as $1/K$; a theoretical justification is derived in the Supplementary Information. Hence, for $P_{DS} \ll 1$, we can make the probability of sampling from the database independent of the number of replicas, replacing f_{max} with f_{max}/K .

We identify two possible strategies for the application of approximate SENS. One is to start sampling from a large database early in the simulation when $E_{on} = E_{max}^{(\text{minima.db})}$, with a small P_{DS} , hence we choose $f_{max} \ll 1$. This procedure allows nested sampling to do most of the work, but ensures that no important basins will be missed. Alternatively, sampling from the database can be delayed until all the high temperature transitions have occurred, at which point we start sampling more extensively from the database, hence $f_{max} \gtrsim 1/2$. Note that the database can be considerably smaller in this case. The first strategy is a slight enhancement to nested sampling, while the latter strategy interpolates between nested sampling and the HSA in a similar spirit to the basin-sampling method [12]. Importantly, even if we sample from the database of minima, we use the MCMC walk to explore more the anharmonic regions of a basin, allowing us to go beyond the harmonic approximation.

RESULTS

We test SENS by calculating the thermodynamic properties of Lennard-Jones clusters exhibiting broken ergodicity. Lennard-Jones (LJ) clusters are systems of particles that interact via the Lennard-Jones potential[52]

$$E = 4\epsilon \sum_{i<j} \left[\left(\frac{\sigma}{r_{ij}} \right)^{12} - \left(\frac{\sigma}{r_{ij}} \right)^6 \right], \quad (9)$$

where ϵ is the pair well depth, σ is the separation at which $E = 0$, and $2^{1/6}\sigma$ is the equilibrium pair separation. LJ clusters have served as benchmarks for many global optimization techniques and thermodynamics sampling [2, 12, 15, 18, 25, 34].

The majority of putative ground states for LJ clusters are based on icosahedral packings [13]. For some *magic number* LJ clusters complete Mackay icosahedra are possible, for examples $N = 13, 55$. Complete icosahedral structures are considerably more stable than neighbouring sizes and their landscape is funneled towards the global minimum [13]. There are, however, other sizes for which the global minimum is not icosahedral. Examples

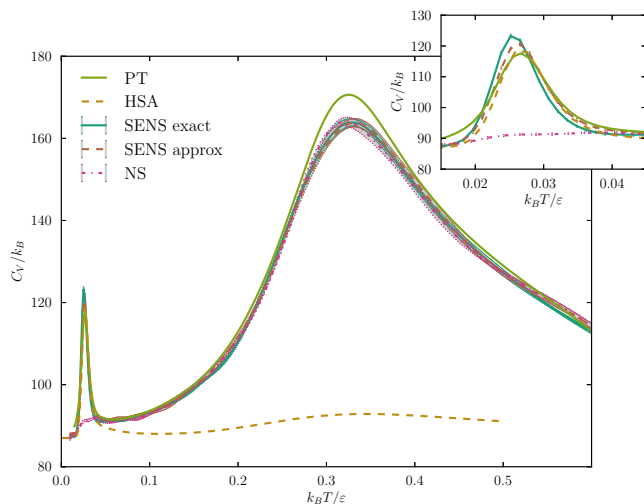


FIG. 1. Heat capacity curves for LJ₃₁. PT and HSA correspond to parallel tempering and the harmonic superposition approximation, respectively. All SENS calculations were performed using $K = 20000$ replicas.

are LJ₃₈, whose ground state is an fcc-truncated octahedron [13], and LJ₇₅ whose global minimum is a Marks decahedron [13]. Due to the overwhelming number (entropic weight) of structures based on incomplete icosahedra at high energy, the energy landscapes of LJ clusters with nonicosahedral global minima exhibit broken ergodicity. Calculating accurate thermodynamic properties for these systems has proved to be a real challenge for all conventional techniques [2, 15, 18, 25] and hybrid or more complicated schemes [12, 14, 15, 18] are necessary. LJ clusters with broken ergodicity therefore provide excellent benchmarks to test the performance of new sampling techniques.

LJ₃₁

LJ₃₁ is the smallest Lennard-Jones cluster exhibiting broken ergodicity and a low temperature solid-solid phase-like transition from Mackay to anti-Mackay surface structures [13]. Convergence of the heat capacity curve for LJ₃₁ by parallel tempering (PT) with 24 geometrically distributed temperatures in the range 0.0125 to 0.6 required $N_E^{total} = 1.9 \times 10^{11}$ energy evaluations to converge (curve shown in Fig. 1). Partay et al. [25] report that $K = 288000$ replicas and $N_E^{total} = 3.4 \times 10^{12}$ energy evaluations were needed to converge the heat capacity curve of LJ₃₁ by nested sampling (NS) using a low particle density of $2.31 \times 10^{-3} \sigma^{-3}$ (100 fold less dense than our system). Fig. 1 compares the heat capacity curves obtained by PT, HSA (computed using $\gtrsim 80000$ minima), NS and SENS for LJ₃₁. The SENS and NS results correspond to $K = 20000$ replicas, $N = 10000$ steps for each MCMC walk, and $\mathcal{P} = 16$ cores. The database of minima used for SENS contained the lowest 183 min-

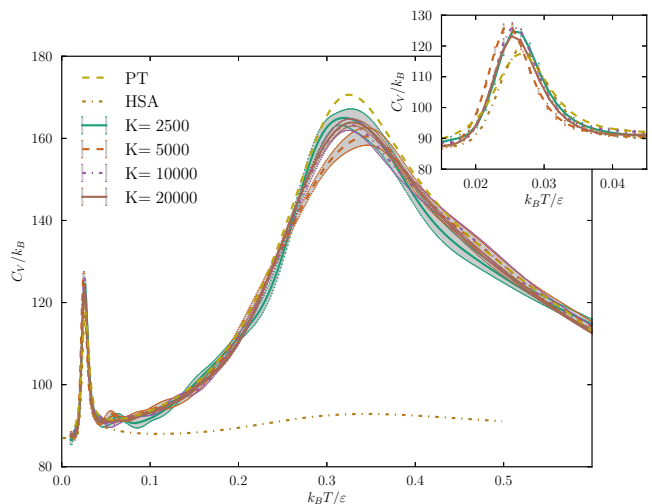


FIG. 2. Comparison of heat capacity curves for LJ₃₁ obtained by exact SENS using different numbers of replicas. The PT and HSA curves were obtained by parallel tempering and the harmonic superposition approximation, respectively.

LJ ₃₁			
Method	K	N	$N_E^{(total)}$
PT			1.9×10^{11}
NS ref.[25]	280000		3.4×10^{12}
NS	20000	10000	1×10^{11}
SENS approx	20000	10000	1×10^{11}
SENS exact	20000	10000	1×10^{11}
SENS exact	10000	10000	5.2×10^{10}
SENS exact	5000	10000	2.6×10^{10}
SENS exact	2500	10000	1.3×10^{10}

TABLE I. Comparison of methods used to obtain the LJ₃₁ heat capacity curves shown in Figs. 1 and 2. $N_E^{(total)}$ indicates the total number of energy evaluations (summed over all processors). PT was performed using 24 replicas spread geometrically through the temperature range 0.0125 to 0.6. Note that approximate SENS can perform as well as exact SENS when fewer replicas are used, in the interest of brevity we do not include these results as the LJ₇₅ calculations illustrate clearly the capabilities of the method.

ima, although for SENS exact we observe that only seven minima contribute to the swaps; see Table IV of Supplementary Information for the swap statistics. From Fig. 1 we see that both exact SENS and approximate SENS are well converged and agree with the PT curve over the whole temperature range, and with the HSA at low temperature. We note that $K = 20000$ replicas are not nearly enough for NS to converge, and the low temperature peak is in fact completely absent. Using this number of replicas SENS requires half the total number of energy evaluations of PT and one order of magnitude less than NS, see Table I. The swap operations do not constitute a noticeable overhead and the reduction in the total number of energy evaluations corresponds to an equivalent

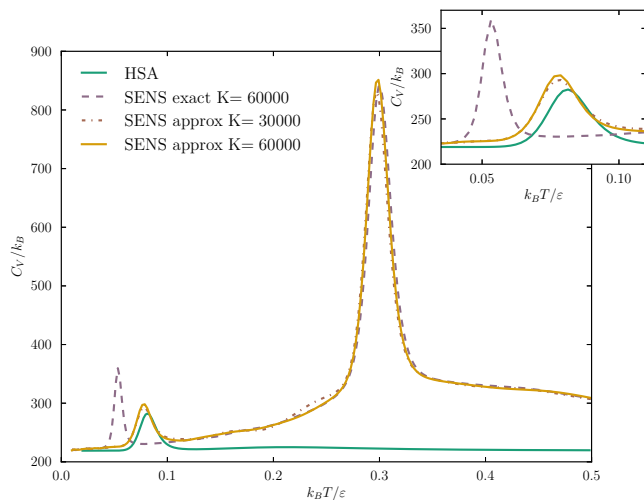


FIG. 3. Heat capacity curves for LJ₇₅. The PT and HSA results were obtained by parallel tempering and the harmonic superposition approximation, respectively. Exact SENS calculations were performed using $K = 60000$ replicas, while results for approximate SENS calculations are shown for both $K = 30000$ and $K = 60000$ replicas.

reduction in wall-clock time.

In Fig. 2 we show a comparison of PT, HSA and exact SENS for a range of replica numbers $2500 \leq K \leq 20000$; see Table I for comparison. We observe that the high temperature peak practically converges for $K = 10000$ and it resembles the features of the converged curve quite well even for smaller numbers of replicas. The low temperature peak instead converges very quickly, for as few as $K = 2500$ replicas, representing an improvement in performance of 20 times over PT. We note that one of the great strengths of SENS is that even when a small number of replicas are used and run times are very short, although the curves may not be completely converged, the physical picture produced by the method is always correct because all the important basins are visited. On the other hand, rapid convergence of the heat capacity curves, requires the HSA to be a good representation for the system. LJ₃₈ is an example for which this condition does not hold as well, see the Supplementary Information for further details.

LJ₇₅

LJ₇₅ is a particularly clear example of a double-funneled energy landscape [13] with $O(10^{25})$ distinct local minima [12]. The decahedral global minimum is separated by a very large potential energy barrier from the lowest icosahedral minimum. Sharapov and Mandelsham [16] showed that $O(10^{12})$ (total) energy evaluations of adaptive parallel tempering are not enough to converge the heat capacity peak corresponding to the solid-solid phase-like transition in LJ₇₅ [16]. Furthermore, the

LJ ₇₅			
Method	K	N	$N_E^{(total)}$
SENS approx	30000	10000	4×10^{11}
SENS approx	60000	10000	8×10^{11}
SENS exact	60000	10000	8×10^{11}

TABLE II. Comparison of methods used to obtain the LJ₇₅ heat capacity curves shown in Fig. 3. $N_E^{(total)}$ indicates the total number of energy evaluations (summed over all processors). PT curves are not shown as the computational cost to converge its heat capacity by this method is computationally prohibitive as shown in Ref. [16]. SENS exact does not converge as quickly as approximate SENS due to the low accuracy of the HSA and hence the low swap acceptance.

rate of convergence slows down dramatically (it practically stops) after $O(10^{11})$ (total) energy evaluations and coupling of PT to the HSA is necessary to obtain convergence of the low temperature peak [16]. Fig. 3 compares the heat capacity curves obtained by HSA (computed using 758 minima) and SENS for LJ₇₅. SENS was carried out using $K = 30000$ or $K = 60000$ replicas and $N = 10000$ steps for each MCMC walk on $\mathcal{P} = 16$ processors. The database of minima for SENS contained the lowest 758 minima. Approximate SENS started sampling from the database at $E_{on} = -369 \epsilon$, while for exact SENS only 10 of the minima contributed to the swaps; see Table VI of the Supplementary Information for swap statistics. Unlike adaptive PT [16], approximate SENS converges in $O(10^{11})$ energy evaluations (Table II), but exact SENS fails to converge the low temperature peak for the same number of replicas. As for LJ₃₈, exact SENS does not converge quickly due to the lower accuracy of the HSA, as inferred from the extremely low swap acceptance (Table VI of Supplementary Information). On the other hand approximate SENS performs considerably better than for LJ₃₈ because the melting transition is well separated from the solid-solid transition, thus allowing sampling from the database relatively early on in the simulation (right after melting) without affecting the melting transition.

Methods

We define a move in MCMC as the displacement of each individual particle along a random vector (n in total). After each MCMC walk we update the step size in order to keep the average acceptance ratio within range of some target value, which we have chosen as 0.5. The default parameter values for the onset function Eq. (8) were $f_{max} \approx 2/3$ and $\Delta E = 1$. We used a spherical box of radius $R = 2.5 \sigma$ for $n = 31$, $R = 2.8 \sigma$ for $n = 38$ and $R = 3.0 \sigma$ for $n = 75$, with no periodic boundary conditions and no cutoff radius. All calculations were carried out on a single workstation with $\mathcal{P} = 16$ processors (eight-core dual Xeon E5-2670 2.6GHz, Westmere) using

the improved parallelization scheme discussed in sec. Parallelization. The calculations were terminated when the energy difference between the replicas with highest and lowest energies was less than $10^{-2} \epsilon$. Energies of the final “live” replicas were added to the output and the compression factor associated with the ℓ^{th} “live” replica was computed as

$$\mu_{\ell}^{(\text{live})} = \prod_{j=0}^{\ell < K} \frac{K - j}{K - j + 1}. \quad (10)$$

Error bars were obtained by the compression factor resampling scheme discussed in the Supplementary Information. By nested sampling or SENS iterations, N_{iter} , we mean a whole nested sampling iteration on \mathcal{P} processors, the total number of energy evaluations is $N_E^{(\text{tot})} = N \times \mathcal{P} \times N_{\text{iter}}$, where N is the number of steps in a MCMC. The computational overhead associated with global optimization by basin-hopping is insignifi-

cant as less than around $O(10^5)$ energy evaluations are necessary to find the global minima of the LJ clusters considered here [35]. Highly modular Python/C parallel implementations of nested sampling and SENS are publicly available [60, 61].

ACKNOWLEDGMENTS

We gratefully acknowledge discussions with Andy Ballard, Victor Rühle, Thomas Stecher, Tine Curk, Boris Fackovec and Robert Baldock. This work has been supported by the European Research Council and the EPSRC. S.M. acknowledges financial support from the Gates Cambridge Scholarship and J.D.S. from the Marie Curie IEF 275544. D.F. acknowledges support from the ERC Advanced Grant 227758, Wolfson Merit Award 2007/R3 of the Royal Society of London.

-
- [1] D. Landau and K. Binder, *A Guide to Monte Carlo Simulations in Statistical Physics* (Cambridge University Press, 2005)
- [2] D. J. Wales, *Energy Landscapes: Applications to Clusters, Biomolecules and Glasses* (Cambridge University Press, 2005)
- [3] G. M. Torrie and J. P. Valleau, “Nonphysical sampling distributions in Monte Carlo free-energy estimation: Umbrella sampling,” *Journal of Computational Physics* **23**, 187–199 (1977)
- [4] B. A. Berg and T. Neuhaus, “Multicanonical ensemble: A new approach to simulate first-order phase transitions,” *Physical Review Letters* **68**, 9–12 (1992)
- [5] F. Wang and D. Landau, “Efficient, Multiple-Range Random Walk Algorithm to Calculate the Density of States,” *Physical Review Letters* **86**, 2050–2053 (2001)
- [6] R. H. Swendsen and J.-S. Wang, “Replica Monte Carlo Simulation of Spin-Glasses,” *Physical Review Letters* **57**, 2607–2609 (1986)
- [7] F. Wang and D. Landau, “Efficient, Multiple-Range Random Walk Algorithm to Calculate the Density of States,” *Physical Review Letters* **86**, 2050–2053 (2001)
- [8] Y. Sugita and Y. Okamoto, “Replica-exchange molecular dynamics method for protein folding,” *Chemical Physics Letters* **314**, 141–151 (1999)
- [9] A. Laio and M. Parrinello, “Escaping free-energy minima,” *Proceedings of the National Academy of Sciences* **99**, 12562–12566 (2002)
- [10] A. Ferrenberg and R. Swendsen, “New Monte Carlo technique for studying phase transitions,” *Physical Review Letters* **61**, 2635–2638 (1988)
- [11] J. D. Chodera, W. C. Swope, J. W. Pitner, C. Seok, and K. A. Dill, “Use of the Weighted Histogram Analysis Method for the Analysis of Simulated and Parallel Tempering Simulations,” *Journal of Chemical Theory and Computation* **3**, 26–41 (2007)
- [12] D. J. Wales, “Surveying a complex potential energy landscape: Overcoming broken ergodicity using basin sampling,” *Chemical Physics Letters* **584**, 1–9 (2013)
- [13] J. P. K. Doye, M. A. Miller, and D. J. Wales, “Evolution of the potential energy surface with size for Lennard-Jones clusters,” *The Journal of Chemical Physics* **111**, 8417 (1999)
- [14] J. P. K. Doye and D. J. Wales, “Thermodynamics of Global Optimization,” *Physical Review Letters* **80**, 1357–1360 (1998)
- [15] P. Poulain, F. Calvo, R. Antoine, M. Broyer, and Ph. Dugourd, “Performances of Wang-Landau algorithms for continuous systems,” *Physical Review E* **73**, 056704 (2006)
- [16] V. A. Mandelshtam, P. A. Frantsuzov, and F. Calvo, “Structural transitions and melting in LJ74-78 lennard-jones clusters from adaptive exchange monte carlo simulations,” *The Journal of Physical Chemistry A* **110**, 5326–5332 (2007)
- [17] V. A. Sharapov and V. A. Mandelshtam, “Solid-solid structural transformations in lennard-jones clusters : Accurate simulations versus the harmonic superposition approximation,” *The Journal of Physical Chemistry A* **111**, 10284–10291 (2007)
- [18] V. A. Sharapov, D. Meluzzi, and V. A. Mandelshtam, “Low-Temperature Structural Transitions: Circumventing the Broken-Ergodicity Problem,” *Physical Review Letters* **98**, 105701 (2007)
- [19] J. Skilling, “Nested sampling for general Bayesian computation,” *Bayesian Analysis* **1**, 833–859 (2006)
- [20] P. Mukherjee, D. Parkinson, and A. R. Liddle, “A Nested Sampling Algorithm for Cosmological Model Selection,” *The Astrophysical Journal* **638**, L51–L54 (2006)
- [21] F. Feroz and M. P. Hobson, “Multimodal nested sampling: an efficient and robust alternative to Markov Chain Monte Carlo methods for astronomical data analyses,” *Monthly Notices of the Royal Astronomical Society* **384**, 449–463 (2008)
- [22] J. R. Shaw, M. Bridges, and M. P. Hobson, “Efficient Bayesian inference for multimodal problems in cosmol-

- ogy,” *Monthly Notices of the Royal Astronomical Society* **378**, 1365–1370 (2007)
- [23] F. Feroz, M. P. Hobson, and M. Bridges, “MultiNest: an efficient and robust Bayesian inference tool for cosmology and particle physics,” *Monthly Notices of the Royal Astronomical Society* **398**, 1601–1614 (2009)
- [24] I. Murray, D. J. C. MacKay, Z. Ghahramani, and J. Skilling, “Nested sampling for Potts models,” *Advances in Neural Information Processing Systems* **18**, 947 (2006)
- [25] L. B. Pártay, A. P. Bartók, and G. Csányi, “Efficient sampling of atomic configurational spaces,” *The Journal of Physical Chemistry B* **114**, 10502–12 (2010)
- [26] S. O. Nielsen, “Nested sampling in the canonical ensemble: Direct calculation of the partition function from NVT trajectories,” *The Journal of Chemical Physics* **139**, 124104 (2013)
- [27] N. S. Burkoff, C. Várnai, S. A. Wells, and D. L. Wild, “Exploring the energy landscapes of protein folding simulations with Bayesian computation,” *Biophysical Journal* **102**, 878–86 (2012)
- [28] L. B. Pártay, A. P. Bartók, and G. Csányi, “Nested sampling for materials: The case of hard spheres,” *Physical Review E* **89**, 022302 (2014)
- [29] B. J. Brewer, L. B. Pártay, and G. Csányi, “Diffusive nested sampling,” *Statistics and Computing* **21**, 649–656 (2010)
- [30] S. Aitken and O. Akman, “Nested sampling for parameter inference in systems biology: application to an exemplar circadian model,” *BMC Systems Biology* **7** (2013)
- [31] R. Dybowski, T. J. McKinley, P. Mastroeni, and O. Restif, “Nested sampling for bayesian model comparison in the context of salmonella disease dynamics,” *PloS one* **8**, e82317 (2013)
- [32] N. Pullen and R. J. Morris, “Bayesian model comparison and parameter inference in systems biology using nested sampling,” *PloS one* **9**, e88419 (2014)
- [33] Z. Li and H. A. Scheraga, “Monte Carlo-minimization approach to the multiple-minima problem in protein folding,” *Proceedings of the National Academy of Sciences of the United States of America* **84**, 6611–5 (1987)
- [34] D. J. Wales and J. P. K. Doye, “Global Optimization by Basin-Hopping and the Lowest Energy Structures of Lennard-Jones Clusters Containing up to 110 Atoms,” *The Journal of Physical Chemistry A* **101**, 5111–5116 (1997)
- [35] M. T. Oakley, R. L. Johnston, and D. J. Wales, “Symmetrisation schemes for global optimisation of atomic clusters,” *Physical Chemistry Chemical Physics* **15**, 3965–3976 (2013)
- [36] D. J. McGinty, “Vapor phase homogenous nucleation and the thermodynamic properties of small clusters of argon atoms,” *The Journal of Chemical Physics* **55**, 580 (1971)
- [37] J. J. Burton, “Vibrational Frequencies and Entropies of Small Clusters of Atoms,” *The Journal of Chemical Physics* **56**, 3133 (1972)
- [38] M. R. Hoare, “Structure and dynamics of simple micro-clusters,” *Advances in Chemical Physics* **40**, 49 (1979)
- [39] F. H. Stillinger and T. A. Weber, “packing structures and transitions in liquids and solids,” *Science* **225**, 983 (1984)
- [40] B. Strodel and D. J. Wales, “Free energy surfaces from an extended harmonic superposition approach and kinetics for alanine dipeptide,” *Chemical Physics Letters* **466**, 105–115 (2008)
- [41] D. J. Wales, “Coexistence in small inert gas clusters,” *Molecular Physics* **78**, 151–171 (1993)
- [42] J. P. K. Doye and D. J. Wales, “An order parameter approach to coexistence in atomic clusters,” *The Journal of Chemical Physics* **102**, 9673 (1995)
- [43] J. P. K. Doye and D. J. Wales, “Calculation of thermodynamic properties of small Lennard-Jones clusters incorporating anharmonicity,” *The Journal of Chemical Physics* **102**, 9659 (1995)
- [44] F. Calvo, J. P. K. Doye, and D. J. Wales, “Characterization of Anharmonicities on Complex Potential Energy Surfaces: Perturbation Theory and Simulation,” *The Journal of Chemical Physics* **115**, 9627–9636 (2001)
- [45] I. Georgescu and V. A. Mandelshtam, “Self-consistent phonons revisited. I. The role of thermal versus quantum fluctuations on structural transitions in large Lennard-Jones clusters,” *The Journal of Chemical Physics* **137**, 144106 (2012)
- [46] The normalised fraction of configuration space $X_i = \Omega_{E \leq E_{\mathcal{R}}} / \Omega_{tot} \in (0, 1)$. Since Nested Sampling assumes uniform sampling in phase space, estimating X_i becomes analogous to estimating the \mathcal{R} -th largest position out of K points sampled at random on a unit segment. The point with \mathcal{R} -th largest position will be distributed on the unit line as $\text{Beta}(K - \mathcal{R} + 1, \mathcal{R})$.
- [47] B. Hartke, “Global optimization,” *Wiley Interdisciplinary Reviews: Computational Molecular Science* **1**, 879–887 (2011)
- [48] D. J. Wales, “Global Optimization of Clusters, Crystals, and Biomolecules,” *Science* **285**, 1368–1372 (1999)
- [49] F. H. Stillinger and T. A. Weber, “Packing structures and transitions in liquids and solids,” *Science* **225**, 983–9 (1984)
- [50] S. Somani and D. J. Wales, “Energy landscapes and global thermodynamics for alanine peptides,” *The Journal of Chemical Physics* **139**, 121909 (2013)
- [51] D. J. Wales and J. P. K. Doye, “Stationary points and dynamics in high-dimensional systems,” *The Journal of Chemical Physics* **119**, 12409–12416 (2003)
- [52] J. E. Lennard-Jones, “Cohesion,” *Proceedings of the Physical Society* **43**, 461–482 (1931)
- [53] R. Zhou and B. J. Berne, “Smart walking: A new method for Boltzmann sampling of protein conformations,” *The Journal of Chemical Physics* **107**, 9185–9196 (1997)
- [54] I. Andricioaei, J. E. Straub, and A. F. Voter, “Smart Darting Monte Carlo,” *The Journal of Chemical Physics* **114**, 6994–7000 (2001)
- [55] K. Mochizuki, C. S. Whittleston, S. Somani, H. Kusumaatmaja, and D. J. Wales, “A conformational factorisation approach for estimating the binding free energies of macromolecules,” *Physical Chemistry Chemical Physics* **16**, 2842–2853 (2014)
- [56] S. W. Olesen, S. N. Fejer, D. Chakrabarti, and D. J. Wales, “A left-handed building block self-assembles into right- and left-handed helices,” *RSC Advances* **3**, 12905–12908 (2013)
- [57] C. J. Forman, S. N. Fejer, D. Chakrabarti, P. D. Barker, and D. J. Wales, “Local Frustration Determines Molecular and Macroscopic Helix Structures,” *The Journal of Physical Chemistry B* **117**, 7918–7928 (2013)
- [58] A. Bunker and B. Dünweg, “Parallel excluded volume tempering for polymer melts,” *Physical Review E* **63**, 016701 (2000)

- [59] H. Fukunishi, O. Watanabe, and S. Takada, "On the Hamiltonian replica exchange method for efficient sampling of biomolecular systems: Application to protein structure prediction," *The Journal of Chemical Physics* **116**, 9058 (2002)
- [60] S. Martiniani and J.D. Stevenson, Nested Sampling(2013), https://github.com/js850/nested_sampling
- [61] S. Martiniani and J.D. Stevenson, Superposition Enhanced Nested Sampling(2013), <https://github.com/smcantab/sens>

Supplementary Information

S.I. A: Sampling configurations in a harmonic well

Given a harmonic potential the configurational density of states for a basin can be obtained by inverse Laplace transforming the configurational partition function. In particular, the scaling goes as:

$$g_c(E) = \mathcal{L}^{-1} \{Z_c(\beta)\} \propto (E_c - V)^{\frac{\kappa}{2}-1}, \quad (\text{A1})$$

where all the terms that do not depend on energy have been left out. $g_c(E)$ is the configurational density of states, Z_c the configurational partition function (evidence), $\beta = 1/k_B T$ is the inverse temperature, E_c the configurational energy, V the potential energy of the corresponding minimum and κ is the number of degrees of freedom (for a n -atoms cluster $\kappa = 3n - 6$). We can write the energy of the simple harmonic oscillator as

$$E_c = V + \frac{1}{2}\xi r^2 \quad (\text{A2})$$

where r is the magnitude of the displacement vector and ξ is the stiffness of the harmonic spring. We want to determine the probability distribution of the configurational energy as a function of the displacement vector norm, $\xi^{\frac{1}{2}}r$, to perform analytical uniform sampling in the harmonic well. The unnormalised probability of finding a configuration between E_c and $E_c + dE_c$ must be proportional to the configurational density of states, from Eq. (A1):

$$p(E_c)dE_c \propto (E_c - V)^{\frac{\kappa}{2}-1}dE_c. \quad (\text{A3})$$

Denoting $q = \xi^{\frac{1}{2}}r$, by a simple change of variables we can express the energy probability distribution in terms of q :

$$p(E_c)dE_c = p(E_c(q))Jdq \propto (q^2)^{\frac{\kappa}{2}-1}dq, \quad (\text{A4})$$

where the Jacobian $J = dE_c/dq = q$ and the equality simplifies to the probability density function

$$p(q)dq \propto q^{\kappa-1}dq. \quad (\text{A5})$$

Hence q must be distributed according to the power law cumulative distribution function $P(q) = q^\kappa$ (denoted $\text{Pow}(\kappa)$) to obtain the correct distribution of energies.

In order to sample uniformly below some energy constraint E_{max} we first generate a random κ -dimensional vector \mathbf{v} with norm $v \sim \text{Pow}(\kappa) \in (0, 1]$ in the unit hypersphere. Then starting from Eq. (A2) we write

$$\mathbf{q}_{usc} = \sqrt{\frac{2(E_{max} - V)}{\xi}} \mathbf{v} \quad (\text{A6})$$

where \mathbf{q}_{usc} is the uniformly sampled configuration vector with energy E_c . It can easily be verified that \mathbf{q}_{usc} has the correct inner product:

$$E_c = \frac{1}{2}\xi q_{usc}^2 = (E_{max} - V)v^2, \quad (\text{A7})$$

where again $v \sim \text{Pow}(\kappa) \in (0, 1]$. The configuration \mathbf{q}_{usc} is then projected onto the orthonormal eigenvector basis $\{\mathbf{e}_i\}$ of the minimum (obtained by diagonalization of the Hessian matrix). The analytically sampled configuration is then:

$$\mathbf{r} = \mathbf{r}_{min} + \sum_{i=1}^{\kappa} \mathbf{q}_i \mathbf{e}_i \quad (\text{A8})$$

where \mathbf{r}_{min} is the configuration of the minimum stored in the database and \mathbf{q}_i is the uniformly sampled configuration in Eq. (A6) with ξ being the eigenvalue associated with the i -th eigenvector, \mathbf{e}_i .

S.I. B: Hamiltonian replica exchange moves satisfy detailed balance

The Hamiltonian replica exchange method associates different Hamiltonians (energy functions) with different replicas of the same system, rather than different temperatures. The detailed balance condition for this method has been derived in Ref. [58, 59].

The probability to accept an exchange between a configuration \mathbf{R}_{sys} , sampled according to an arbitrary system Hamiltonian \mathbb{H}_{sys} , and a configuration \mathbf{R}_{har} sampled according to a harmonic Hamiltonian \mathbb{H}_{har} is:

$$P(\mathbf{R}_{sys} \rightarrow \mathbf{R}_{har}) = \min\left(1, e^{-\beta(E_{after} - E_{before})}\right), \quad (\text{B1})$$

where

$$E_{before} = \mathbb{H}_{sys}(\mathbf{R}_{sys}) + \mathbb{H}_{har}(\mathbf{R}_{har}), \quad (\text{B2})$$

$$E_{after} = \mathbb{H}_{sys}(\mathbf{R}_{har}) + \mathbb{H}_{har}(\mathbf{R}_{sys}). \quad (\text{B3})$$

In SENS we effectively sample configurations at infinite temperature ($\beta \rightarrow 0$), with a hard constraint in energy at E_{max} which can be cast into the Hamiltonian so that

$$\mathbb{H}'_x(\mathbf{R}_y) = \begin{cases} \mathbb{H}_x(\mathbf{R}_y) & \text{if } \mathbb{H}_x(\mathbf{R}_y) \leq E_{max} \\ \infty \equiv E_{barrier} & \text{if } \mathbb{H}_x(\mathbf{R}_y) > E_{max} \end{cases}$$

and we require that

$$1/\beta \gg \mathbb{H}_{sys}(\mathbf{R}_{sys}), \mathbb{H}_{har}(\mathbf{R}_{har}). \quad (\text{B4})$$

Therefore, if either $\mathbb{H}_{sys}(\mathbf{R}_{har})$ or $\mathbb{H}_{har}(\mathbf{R}_{sys})$ diverges, E_{after} will diverge such that $\beta E_{after} = \infty$. This last condition requires that

$$E_{barrier} \gg 1/\beta. \quad (\text{B5})$$

It follows that Eq. (7) is the correct condition for a swap and that detailed balance holds.

$$p_b(i) = \frac{\Omega_c^{(b)}}{\Omega_c^{(a)} + \Omega_c^{(b)}} = \frac{(E_i - V_b)^{\frac{\kappa}{2}} \Theta(E_i - V_b) \prod_{\alpha=1}^{\kappa} \nu_{\alpha}^{(a)} o_a}{(E_i - V_b)^{\frac{\kappa}{2}} \Theta(E_i - V_b) o_a \prod_{\alpha=1}^{\kappa} \nu_{\alpha}^{(a)} + (E_i - V_a)^{\frac{\kappa}{2}} \Theta(E_i - V_a) o_b \prod_{\alpha=1}^{\kappa} \nu_{\alpha}^{(b)}}. \quad (\text{C2})$$

S.I. C: Onset function scaling

How well would SENS perform in a multifunneled landscape? Let us assume that SENS is using a database that stores the lowest minima m_a and m_b of two different funnels, with associated energies V_a and V_b , respectively. Assuming that funnel F_b has already been missed (F_b is not populated and E_{max} is lower than the lowest transition state that leads to F_b) and all replicas are already in funnel F_a , the probability of successfully sampling in F_b is then

$$\Pr(\text{success} | K \text{ replicas in } F_a) = 1 - \prod_{i=1}^n (1 - P_{DS} p_b(i))^{\mathcal{P}}, \quad (\text{C1})$$

where n is the number of iterations before the calculation terminates, \mathcal{P} is the number of processors, P_{DS} is a user defined probability of sampling from the database, and $p_b(i)$ is the discrete probability density that the minimum sampled from the database is m_b . Assuming that the funnels are harmonic we obtain Eq. (C2) where $\nu_{\alpha} = \omega_{\alpha}/(2\pi)$ is the vibrational frequency of mode α and for an object corresponding to a point group with o independent symmetry operations, there are o permutation-inversion operations associated with barrierless reorientations [2]. The ideal value for P_{DS} must then satisfy an identity of the form

$$1 - \prod_{i=1}^{n(V_a)} (1 - P_{DS} p_b(i))^{\mathcal{P}} = \phi, \quad (\text{C3})$$

where $n(V_a)$ is the average number of steps necessary for descending from E_g to V_a and ϕ is a probability close to 1, say $\phi = 0.999$. Taking the logarithm of both sides, Eq. (C3) can be rewritten as

$$\sum_{i=1}^{n(V_a)} \log(1 - P_{DS} p_b(i)) = \frac{\log(1 - \phi)}{\mathcal{P}}. \quad (\text{C4})$$

For small P_{DS} linearisation then leads to

$$P_{DS} = -\frac{\log(1 - \phi)}{\mathcal{P} \sum_{i=1}^{n(V_a)} p_b(i)}, \quad (\text{C5})$$

which provides an optimal value for P_{DS} . To calculate the average number of steps necessary to descend a harmonic basin, first we calculate an expression for the set of energies that would be obtained by nested sampling if at each step the configurational space was compressed exactly by μ . We note that

$$\mu = \frac{\Omega(E_{i+1})}{\Omega(E_i)} = \frac{(E_{i+1} - V)^{\frac{\kappa}{2}}}{(E_i - V)^{\frac{\kappa}{2}}} \quad (\text{C6})$$

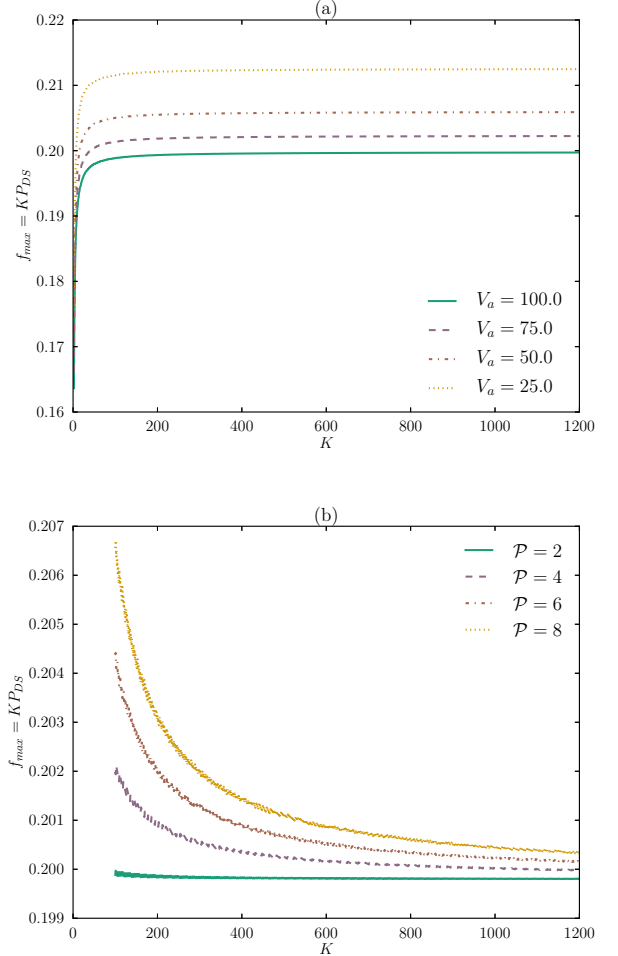


FIG. 4. Eq. (C8) gives the average number of steps necessary to descend a particular harmonic basin as a function of the number of replicas K and by substituting it in Eq. (C3) we can evaluate P_{DS} , the optimal probability of sampling from the database of minima. As long as K is sufficiently large, $f_{max} = KP_{DS}$ will be approximately constant, hence the optimal P_{DS} scales as $1/K$. (a) As V_a , the potential of m_a , decreases, the volume of F_a increases, and hence the optimal f_{max} increases as well. (b) The optimal f_{max} should be independent of the number of processors used, hence for sufficiently large K all curves approach the same value. Unless specified assume $\mathcal{P} = 1$, $\kappa = 3$, $E_g = 500$, $V_a = 100$, $V_b = 0$, $v_{\alpha}^{(a)} = 1$, $v_{\alpha}^{(b)} = 10$, $o_b = o_a = 1$, $\delta = 10$, $\phi = 0.999$.

from which we find

$$E_i = (E_0 - V)\mu^{\frac{2i}{\kappa}} + V, \quad (\text{C7})$$

where $\mu = 1 - \mathcal{P}/(K + 1)$. The number of steps $n(V_a)$ necessary to descend from E_g to $E - V_a = 10^{-\delta}$ can be

obtained by rearranging Eq. (C7) to give

$$n(V_a) = -\frac{\kappa \delta \log(10) + \log(E_g - V_a)}{2 \log(\mu)}. \quad (\text{C8})$$

Finally, substituting Eq. (C7) for E_i in Eq. (C2) we can evaluate Eq. (C3) numerically to obtain an optimal value for P_{DS} (approximating $n(V_a)$ to the nearest integer).

In the main text we introduce the onset function Eq. (8) and suggest that for small P_{DS} an optimal way to make the probability of sampling from the database of minima independent of the number of replicas, is to use the prefactor $1/K$, hence the maximum frequency to sample from the minima, should be f_{max}/K , where f_{max} is a user-defined parameter. Eq. (C8) gives the average number of steps necessary to descend a particular harmonic basin as a function of the number of replicas and by substituting this result in Eq. (C3) we can evaluate P_{DS} , the optimal probability of sampling from the database of minima. In Fig. C we plot $f_{max} = KP_{DS}$ vs K . For large K the optimal value of sampling from the minima scales as $1/K$, thus justifying the use of the prefactor in the onset function.

S.I. D: Algorithms

1. SENS

A complete pseudo-code implementation of the SENS algorithm is provided in Algorithm 3.

```

▷ initialisation, set  $i = 0$ 
1: generate a database of minima in minima.db ;
2: for minimum in minima.db do
3:   compute the Hessian matrix and its eigenvalues
   (needed to compute the HSA weight);
4: end for
5: while  $i < K$  do
6:   sample a random configuration of the system;
7:   store its coordinates and its energy in LiveList ;
8: end while
▷ main loop
9: while termination condition is False do
10:  remove the  $\mathcal{P}$  replicas  $\{\mathbf{R}_m^{(1)}, \dots, \mathbf{R}_m^{(\mathcal{P})}\} \equiv \{\mathbf{R}_m\}$  with
   highest energy  $\{E_m^{(1)} > \dots > E_m^{(\mathcal{P})}\} \equiv \{E_m\}$ 
   from LiveList ;
11:  append  $\{E_m\}$  to OutputList ;
12:  set  $E_{max} = E_m^{(\mathcal{P})}$  ;
13:  sample  $\mathcal{P}$  replicas  $\{\mathbf{R}_s^{(1)}, \dots, \mathbf{R}_s^{(\mathcal{P})}\} \equiv \{\mathbf{R}_s\}$  from
   LiveList at random;
14:  add a copy of  $\{\mathbf{R}_s\}$  to LiveList ;
15:  MCLoop  $\{\{\mathbf{R}_s\}, \text{minima.db}, E_{max}\}$  ;
16: end while
17: append LiveList to OutputList ;

```

ALGORITHM 3. Superposition Enhanced Nested Sampling

2. Exact SENS

A pseudo-code implementation of the MCLoop function for exact SENS can be found in Algorithm 4.

```

1: for all  $\mathbf{R}_s$  in  $\{\mathbf{R}_s\}$  do
2:   sample a minimum  $m$  from minima.db according to
   its HSA entropic weight;
3:   analytically generate a configuration  $\mathbf{R}_{har}$  in
   the harmonic well of  $m$ , with energy
    $\mathbb{H}_{har}(\mathbf{R}_{har}) = E_{har}^{(\mathbf{R}_{har})}$ ;
4:   evaluate  $\mathbb{H}_{sys}(\mathbf{R}_{har}) = E_{sys}^{(\mathbf{R}_{har})}$ 
   and  $\mathbb{H}_{har}(\mathbf{R}_s) = E_{har}^{(\mathbf{R}_s)}$ 
5:   if  $E_{har}^{(\mathbf{R}_s)} \leq E_{max}$  and  $E_{sys}^{(\mathbf{R}_{har})} \leq E_{max}$  then
6:     swap  $\mathbf{R}_{har} \leftrightarrow \mathbf{R}_s$ ;
7:     for  $l = 0$  to  $N$ -steps do
8:       walk  $\mathbf{R}_s$  by sampling uniformly within
        $\{E_s\} \leq E_{max}$ ;
9:     end for
10:    else reject the swap and perform a standard MCMC;
11:    end if
12: end for

```

ALGORITHM 4. Exact SENS MCLoop

The energy of a configuration \mathbf{R}_s with respect to \mathbf{R}_{min} is

$$E_{har}^{(\mathbf{R}_s)} = E_{har}^{(\mathbf{R}_{min})} + (\mathbf{R}_s - \mathbf{R}_{min})^\top \mathcal{H}_{min}(\mathbf{R}_s - \mathbf{R}_{min}), \quad (\text{D1})$$

where \mathcal{H}_{min} is the Hessian matrix associated with \mathbf{R}_{min} . Note that more careful considerations are needed when dealing with Lennard-Jones clusters, in fact \mathbf{R}_{min} is fixed in the database (hence also \mathcal{H}_{min}), thus breaking the translational and rotational invariance of the system. In order to avoid this problem we can either align \mathbf{R}_{min} to \mathbf{R}_s , but then \mathcal{H}_{min} must also be recalculated, or we can do the opposite, which is the most efficient solution. A pseudo-code implementation of the MCLoop function specific to this system is provided in Algorithm 5.

3. Approximate SENS

A pseudo-code implementation of the MCLoop function for approximate SENS is presented in Algorithm 6.

▷ this loop is performed in parallel

```

1: for all  $\mathbf{R}_s$  in  $\{\mathbf{R}_s\}$  do
2:   sample a minimum  $m$  from minima.db according to
   its HSA entropic weight;
3:   analytically generate a configuration  $\mathbf{R}_{har}$  in
   the harmonic well of  $m$ , with energy
    $\mathbb{H}_{har}(\mathbf{R}_{har}) = E_{har}^{(\mathbf{R}_{har})}$ ;
4:   evaluate  $\mathbb{H}_{LJ}(\mathbf{R}_{har}) = E_{LJ}^{(\mathbf{R}_{har})}$ ;
5:   if  $E_{LJ}^{(\mathbf{R}_{har})} > E_{max}$  then
6:     reject the exchange and perform a standard
     MCMC;
7:   else
8:     quench  $\mathbf{R}_s \rightarrow \mathbf{R}_{que}$  with energy
      $\mathbb{H}_{LJ}(\mathbf{R}_{que}) = E_{LJ}^{(\mathbf{R}_{que})}$  and find the minimum
     configuration  $\mathbf{R}_{min}$  with the corresponding energy
     in minima.db ;
9:     find the set of permutations ( $\mathcal{P}$ ) and rotations ( $\mathcal{R}$ )
     such that  $\mathcal{P}\mathcal{R}\mathbf{R}_{que} = \mathbf{R}_{min}$ ;
10:    generate  $\mathbf{R}_s^{(\mathcal{P}\mathcal{R})} = \mathcal{P}\mathcal{R}\mathbf{R}_s$ , which is now aligned
    to  $\mathbf{R}_{min}$ ;
11:    compute  $\mathbb{H}_{har}(\mathbf{R}_s^{(\mathcal{P}\mathcal{R})}) = E_{har}^{(\mathbf{R}_s^{(\mathcal{P}\mathcal{R})})}$ ;
12:    if  $E_{har}^{(\mathbf{R}_s^{(\mathcal{P}\mathcal{R})})} > E_{max}$  then
13:      reject the move and perform a standard
      MCMC;
14:    else swap  $\mathbf{R}_{har} \leftrightarrow \mathbf{R}_s$ ;
15:      for  $l = 0$  to  $N$ -steps do
16:        walk  $\mathbf{R}_s$  by sampling uniformly within
         $\{E_s\} \leq E_{max}$ ;
17:      end for
18:    end if
19:  end if
20: end for

```

ALGORITHM 5. Exact SENS MCLoop for LJ-clusters

```

for all  $\mathbf{R}_s$  in  $\{\mathbf{R}_s\}$  do
  sample a minimum configuration  $\mathbf{R}_b$  from minima.db
  according to its HSA entropic weight;
  if  $u \sim \text{Uniform}(0, 1) < P_{DS}$  then
    swap  $\mathbf{R}_b \leftrightarrow \mathbf{R}_s$ ;
    for  $l = 0$  to  $N$ -steps do
      walk  $\mathbf{R}_s$  by sampling uniformly within
       $\{E_s\} \leq E_{max}$ ;
    end for
  else reject the swap and perform a standard MCMC;
  end if
end for

```

ALGORITHM 6. Approximate MCLoop

S.I. E: Statistical Uncertainty by Compression Factor Resampling

The nested sampling algorithm produces as its primary product a list of parameters (in our case energies) with an associated fraction of configurational space $X_i = \prod_{j=0}^i t_j$, where the t_j are the compression factors sampled on a unit interval with probability distribution $\text{Beta}(K - \mathcal{P} + 1, \mathcal{P})$ and expectation value

$\mu = 1 - \mathcal{P}/(K + 1)$. The exploration of configuration space is the challenging and time consuming part of the algorithm, while the overhead due to the assignment of compression factors is almost irrelevant. In general we use the expectation value μ of these compression factors in order to find the bins of density of states, g , that we need to calculate thermodynamic properties. Given a set of energies obtained by nested sampling, the correct size of the bins for the density of states is one unique realisation of the compression factors t that we do not know a priori (it is for this reason that we use the expectation value μ). There is some statistical uncertainty associated with the distribution of the bin size, which is ultimately due to the distribution of compression factors t , which we know. Since we are interested in the distribution of some observable $Q(\mathbf{E})$, say the heat capacity, we can use a representative set of parameters $\tilde{\mathbf{E}} = \tilde{E}_1, \tilde{E}_2, \dots, \tilde{E}_n$ (energies) obtained by nested sampling (the time consuming part) and sample c sets of compression factors $\mathbf{t}_\ell = t_1^{(\ell)}, t_2^{(\ell)}, \dots, t_n^{(\ell)}$ to associate with this representative set of parameters. This procedure is justified by the fact that we are interested in the probability distribution of $Q(\tilde{\mathbf{E}})$ given the joint probability distribution $p(\mathbf{t}_\ell) = p(t_1^{(\ell)})p(t_2^{(\ell)}) \dots p(t_n^{(\ell)})$. The mean and variance of $Q(\tilde{\mathbf{E}})$ are therefore

$$\langle Q(\tilde{\mathbf{E}}) \rangle = \sum_{\ell=1}^c Q(\tilde{\mathbf{E}})p(\mathbf{t}_\ell) = \frac{1}{c} \sum_{\ell=1}^c Q(\tilde{\mathbf{E}}|\mathbf{t}_\ell); \quad (\text{E1})$$

$$\begin{aligned} \text{Var} \left(Q(\tilde{\mathbf{E}}) \right) &= \sum_{\ell=1}^c Q(\tilde{\mathbf{E}})^2 p(\mathbf{t}_\ell) - \left(\sum_{\ell=1}^c Q(\tilde{\mathbf{E}})^2 p(\mathbf{t}_\ell) \right)^2 \\ &= \frac{1}{c} \sum_{\ell=1}^c Q(\tilde{\mathbf{E}}|\mathbf{t}_\ell)^2 - \left(\frac{1}{c} \sum_{\ell=1}^c Q(\tilde{\mathbf{E}}|\mathbf{t}_\ell) \right)^2. \end{aligned} \quad (\text{E2})$$

A protocol for quantifying uncertainty of this form was already suggested by Skilling [19]. However, this method suffers from some flaws: it does not include an estimate of systematic uncertainties and does not include in any way an estimate of the uncertainty due to the incomplete sampling of configurational space. The latter effect is due to the fact that resampling is performed over one representative set of energies ($\tilde{\mathbf{E}}$) that could be missing a whole part of configurational space.

S.I. F: Results

1. LJ₃₈

LJ₃₈ has a double-funnel energy landscape [43] and its heat capacity exhibits three peaks: the first high temperature peak corresponds to a vapour-liquid transition,

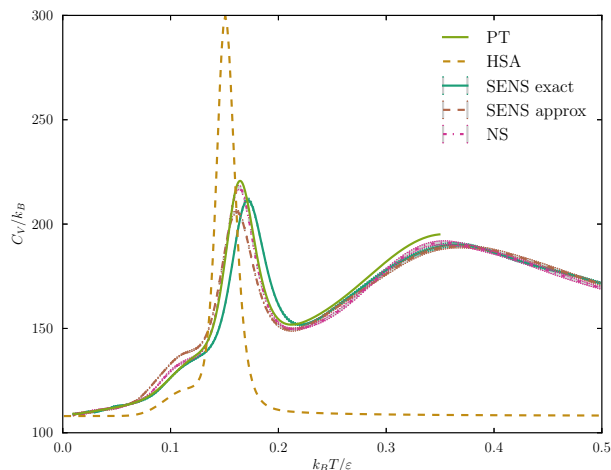


FIG. 5. Heat capacity curves for LJ₃₈. The PT and HSA results were obtained by parallel tempering and the harmonic superposition approximation, respectively.

the second peak corresponds to melting, and the low temperature peak corresponds to a solid-solid transition from the cuboctahedral global minimum to the lowest icosahedral minimum [14]. The PT heat capacity curve for LJ₃₈ generally overestimates the temperature at which the solid-solid phase-like transition occurs and, consequently, disappears under the melting peak, and should appear, instead, as a small shoulder slightly under the melting peak [15, 17]. For this reason long calculations are necessary for the heat capacity to converge. Partay et al. [28] employed $K = 244000$ replicas and $O(10^{12})$ energy evaluations to resolve the heat capacity of LJ₃₈ by NS. Fig. 5 compares the heat capacity curves obtained by PT (using a box of radius $R = 2.8 \sigma$), HSA (computed using $\gtrsim 89000$ minima) and SENS for LJ₃₈. SENS was carried out using $K = 50000$ replicas and $N = 10000$ steps for each MCMC walk. The database of minima used for SENS contained approximately 89000 minima. It appears that neither version of SENS can outperform NS or parallel tempering, which require the same number of energy evaluations to converge; see Table III for comparison. Exact SENS fails due to the inaccuracy of the HSA, and Table V shows the number of effective swaps from and to the basin. These numbers are considerably smaller than for LJ₃₁ (see Table IV), even if the total number of iterations for LJ₃₈ is much larger. Approximate SENS should generally work independently of the quality of the HSA. Here, however, the three transitions overlap significantly thus preventing sampling from the database early enough to get the right low temperature behaviour without affecting the high temperature behaviour. This is not the case for LJ₇₅ where the phase-like transitions are well separated in temperature and sampling can start early enough to get the correct low temperature behaviour without affecting the melting transition.

LJ ₃₈			
Method	K	N	$N_E^{(total)}$
PT			$O(10^{11})$
NS ref.[28]	244000		$O(10^{12})$
NS	50000	10000	3.3×10^{11}
SENS approx	50000	10000	3.3×10^{11}
SENS exact	50000	10000	3.3×10^{11}

TABLE III. Comparison of methods used to obtain the LJ₃₁ heat capacity curves shown in Fig. 5. $N_E^{(total)}$ indicates the total number of energy evaluations (summed over all processors).

2. Swap statistics in exact SENS calculations

In this section we present statistics for the exact SENS swaps in the longest runs of each LJ system presented in the paper. For each minimum we report the total number of swaps that led to this minimum, the number of effective swaps to this minimum (thus excluding the swaps within the same minimum) and the number of effective swaps that led from the minimum to another.

LJ ₃₁			
minimum	total swaps to	effective swaps from	effective swaps to
-133.586421919	346376	4225	5994
-133.293821966	14585	7167	5403
-133.183574005	1529	1325	1325
-133.104620445	412	385	365
-132.998423589	25	11	25
-132.801757275	1	0	1
-132.765536037	0	1	0
-132.721370719	1	0	1

TABLE IV. Number of swaps to and from basins in exact SENS for LJ₃₁ using $K = 20000$ replicas, $N = 10000$ steps for each MCMC and $\mathcal{P} = 16$. Total number of iterations per processor= 650025.

LJ ₃₈			
minimum	total swaps to	effective swaps from	effective swaps to
-173.928426591	486584	245	48
-173.252378416	65	26	63
-173.134317009	163	27	154
-172.958633408	4	2	4
-172.877736411	38	6	37
-172.234926493	0	1	0
-171.992596189	1	0	1

TABLE V. Number of swaps to and from basins in exact SENS for LJ₃₈ using $K = 50000$ replicas, $N = 10000$ steps for each MCMC and $\mathcal{P} = 16$. Total number of iterations per processor= 2082691.

LJ ₇₅			
minimum	total swaps to	effective swaps from	effective swaps to
-397.492330983	632019	1	704
-396.282248826	15	296	12
-396.238512215	14	270	10
-396.193034959	7	41	5
-396.192994186	3	11	3
-396.191648856	4	45	4
-396.186860193	0	1	0
-396.126268882	2	63	1
-396.061061075	1	0	1
-396.061598578	0	13	0
-396.061061075	0	1	0
-396.057293139	1	0	1
-395.992783183	1	0	1

TABLE VI. Number of swaps to and from basins in exact SENS for LJ₇₅ using $K = 60000$ replicas, $N = 10000$ steps for each MCMC and $\mathcal{P} = 16$. Total number of iterations per processor= 5043100.